

A w phantom transition at $z_t < 0.1$ as a resolution of the Hubble tension

George Alestas,^{1,*} Lavrentios Kazantzidis,^{1,†} and Leandros Perivolaropoulos^{1,‡}

¹*Department of Physics, University of Ioannina, GR-45110, Ioannina, Greece*

(Dated: March 10, 2022)

A rapid transition of the dark energy equation of state parameter w at a transition redshift $z_t < 0.1$ from $w \simeq -1$ at $z > z_t$ to $w < -1$ at $z < z_t$ can lead to a higher value of the Hubble constant while closely mimicking a Planck18/ Λ CDM form of the comoving distance $r(z) = \int_0^z \frac{dz'}{H(z')}$ for $z > z_t$. Such a Late w Phantom Transition (*LwPT*) avoids the discontinuity of $H(z)$ suggested in previous studies and thus does not require a step in the Pantheon Hubble diagram which is strongly constrained. We demonstrate that such an ultra low z abrupt feature of $w(z)$ provides a better fit to cosmological data compared to smooth late time deformations of $H(z)$ that also address the Hubble tension. The strongly present day phantom dark energy behavior implied by this class of models hints towards a rapid approach of a Big Rip singularity which for $z_t = 0.02$ will rip the universe in less than 3.5 billion years. Early hints of such effect may be observable in the dynamics of the nearest and largest bound systems (*e.g.* Virgo structures). The *LwPT* can be generically induced by a phantom scalar field frozen by Hubble friction mimicking the cosmological constant and currently entering its ghost instability phase as Hubble friction decreases below the field dynamical scale.

I. INTRODUCTION

The cosmological comoving distance to redshift z defined in a flat universe as $r(z) = \int_0^z \frac{dz'}{H(z')}$ where $H(z)$ is the Hubble expansion rate has been constrained to a level of about 2% using standard candles (SnIa calibrated with Cepheid stars [1–3] and Red Giant stars [4, 5] or megamassers in accretion disks [6]), a standard ruler (the sound horizon at last scattering calibrated using the CMB anisotropy spectrum [7, 8] and/or Big Bang Nucleosynthesis (BBN) [9]), strong gravitational lensing [10, 11] and gravitational waves [12, 13]. The comoving distance determined using calibrated standard candles at $z < 0.23$ is offset with the comoving distance determined using the sound horizon standard ruler at $z > 0.23$, by about 9% which corresponds to a tension of about 5σ . In the context of a Planck18/ Λ CDM form of $H(z)$ this mismatch of $r(z)$ becomes realized as a mismatch of the values of the Hubble constant determined by the two methods [14, 15].

Despite of intense efforts [16–19] it has not been possible to reliably identify systematic errors of the calibrators used in the context of the two methods. For example parallax data from Gaia have recently confirmed [20, 21] the calibration of Cepheid stars while attempts to recalibrate the sound horizon assuming *e.g.* neutrino self interactions [22] or early dark energy [23–29] have produced new tensions with other cosmological data [30, 31] (including growth rate from weak lensing [32–35] and peculiar velocities [36–41]). It therefore becomes increasingly probable that the mismatch in the high- z -low- z form of $r(z)$ is indeed a physical effect that will require deformation of $H(z)$ from its Planck18/ Λ CDM form.

Attempts to consider smooth deformations of $H(z)$

[42–48] at $z \simeq O(1)$ have been successful in matching $r(z_{rec})$ with $r(z=0)$ but have been unable to match the value of $r(z \simeq O(1))$ which is strongly constrained by BAO and SnIa data to be close to the form indicated by Planck18/ Λ CDM.

A remaining possibility is that of an abrupt deformation of $H(z)$ at $z \lesssim 0.1$ ($H(z)$ transition). Such a deformation has been considered in previous studies [49–51] as a discontinuity of $H(z)$ occurring at $z_t < 0.1$. It was shown however, that if such a feature occurs at $z_t < 0.01$ *i.e.* below the redshift where Hubble flow starts, it would be undetectable by standard candles [50] and thus it would not be able to justify the measured decreased value of $r(z)$ at low z . On the other hand, if it occurred at $0.01 < z_t < 0.1$ with the proper amplitude to reduce $r(z)$ to the required level, it would have to produce a step-like feature in the SnIa Hubble diagram with amplitude $\Delta m = 0.2$. A discontinuity with such an amplitude is inconsistent with the Pantheon data. It is therefore clear that even though the existence of a feature in the form of $H(z)$ at $z_t < 0.1$ is likely, this feature would need to be smoother than a discontinuity. Such a feature could occur at redshifts as low as $z_t \simeq 0.02$ without significantly affecting the locally determined value of H_0 [51]. In the present analysis we propose such a feature in the form of a discontinuity of the equation of state parameter $w(z)$ rather than a discontinuity of $H(z)$ [52, 53].

In particular, we consider a transition of $w(z)$ as

$$w(z) = -1 + \Delta w \Theta(z_t - z) \quad (1.1)$$

which implies a Hubble expansion rate $h(z) \equiv H(z)/100 \text{ km}/(\text{sec Mpc})$ of the form

* g.alestas@uoi.gr

† l.kazantzidis@uoi.gr

‡ leandros@uoi.gr

$$\begin{aligned}
h_w(z)^2 &\equiv \omega_m(1+z)^3 + \omega_r(1+z)^4 + (h^2 - \omega_m - \omega_r) \left(\frac{1+z}{1+z_t} \right)^{3\Delta w} & z < z_t \\
h_w(z)^2 &\equiv \omega_m(1+z)^3 + \omega_r(1+z)^4 + (h^2 - \omega_m - \omega_r) & z > z_t
\end{aligned} \tag{1.2}$$

where $\omega_m \equiv \Omega_{0m}h^2$, $\omega_r \equiv \Omega_{0r}h^2$ are the matter and radiation density parameters assumed fixed to their Planck18/ Λ CDM values in the next section. In what follows we assume $0.01 < z_t < 0.1$ and define $h_{local} \equiv 0.74$ and $h_{CMB} \equiv 0.674$ which correspond to the Hubble constant values obtained with local standard candle measurements of $r(z)$ and sound horizon standard ruler measurements in the context of Planck18/ Λ CDM respectively.

In the context of the above Late w Phantom Transition ($LwPT$) model the following interesting questions emerge:

- What is the functional form of $\Delta w(z_t)$ so that $h(z=0) = h_{local}$ as implied by local measurements while maintaining the required Planck18/ Λ CDM form of $r(z)$ for $z \gg z_t$?
- How closely does the $LwPT$ model reproduce the form of the Planck18/ Λ CDM comoving distance $r(z)$ for $z > z_t$? How does this form of $r(z)$ compare with the corresponding form of the $H(z)$ transition?
- How does the quality of fit of the $LwPT$ model to cosmological data (CMB, SnIa, BAO and SH0ES) compare with the corresponding quality of fit of typical models that utilize smooth deformations of $H(z)$ to address the H_0 tension.
- What are the favored values of Δw and what are the implications for the future evolution of the universe?

In the present analysis we address the above questions. The structure of this paper is the following: In the next section we investigate analytically the ability of the $LwPT$ model (1.2) to reproduce the Planck18/ Λ CDM form of the comoving distance for $z > z_t$ while keeping $h(z=0) = 0.74$. We also identify the values $\Delta w(z_t)$ that achieve this goal using an analytical approach. In section III we use cosmological data (CMB, SnIa, BAO and SH0ES) to identify the best fit w_0, w_a, Ω_{0m} parameter values for various transition redshifts z_t and identify the improvement of the quality of fit as z_t decreases down to the minimum acceptable value $z_t \simeq 0.02$. We also compare this quality of fit to the data with the Planck18/ Λ CDM model (without the SH0ES datapoint) and with a typical smooth $H(z)$ deformation model ($wCDM$) that is designed to address the Hubble tension. Finally in section IV we summarize the main results of our analysis and discuss the implications of these results for the future evolution of the universe if this model is in-

deed realized in Nature. We also discuss possible future extensions of this analysis.

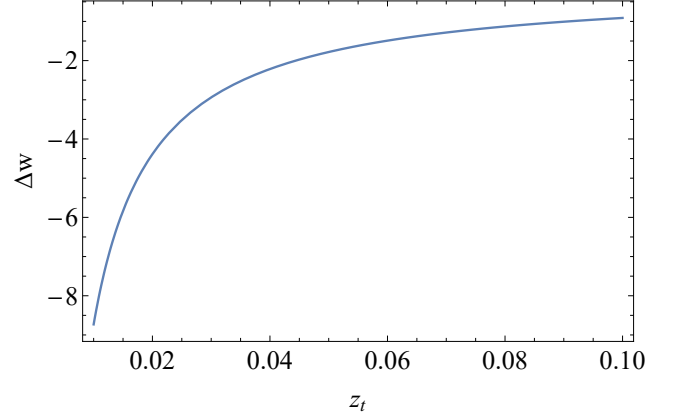


FIG. 1. The equation of state shift Δw required for $h_w(z=0) = h_{local}$ as a function of the transition redshift z_t . Notice the strongly phantom behavior of the dark energy equation of state $w = -1 - \Delta w$ for $z < z_t$.

II. THE COSMOLOGICAL COMOVING DISTANCE IN THE $LwPT$ MODEL

In order to fix the parameters ω_m, ω_r, h and Δw in the $LwPT$ ansatz (1.2) we impose the following conditions:

- It should reproduce the comoving distance corresponding to Planck18/ Λ CDM r_Λ for $z \gg z_t$ where

$$r_\Lambda(z) \equiv \int_0^z \frac{dz'}{\omega_m(1+z')^3 + \omega_r(1+z')^4 + (h^2 - \omega_m - \omega_r)} \tag{2.1}$$

where $\omega_m \equiv \Omega_{0m}h^2 = 0.143$, $\omega_r \equiv \Omega_{0r}h^2 = 4.64 \times 10^{-5}$ and $h = h_{CMB} = 0.674$.

- It should reproduce the local measurements of the Hubble parameter

$$h_w(z=0) = h_{local} = 0.74. \tag{2.2}$$

The first condition fixes the parameters ω_m, ω_r and h to their Planck18/ Λ CDM best fit values. Since we consider $z_t < 0.1 \ll 1$ it is straightforward to obtain an upper bound for the relative difference

$$\frac{\Delta r}{r}(z) \equiv \frac{r_w(z) - r_\Lambda(z)}{r_\Lambda(z)} < \frac{h_{local} - h_{CMB}}{h_{CMB}} \simeq 0.1 \tag{2.3}$$

where $r_w(z) \equiv \int_0^z \frac{dz'}{h_w(z')}$ is the comoving distance corresponding to the $LwPT$ model (1.2). $\frac{\Delta r}{r}(z)$ is maximum

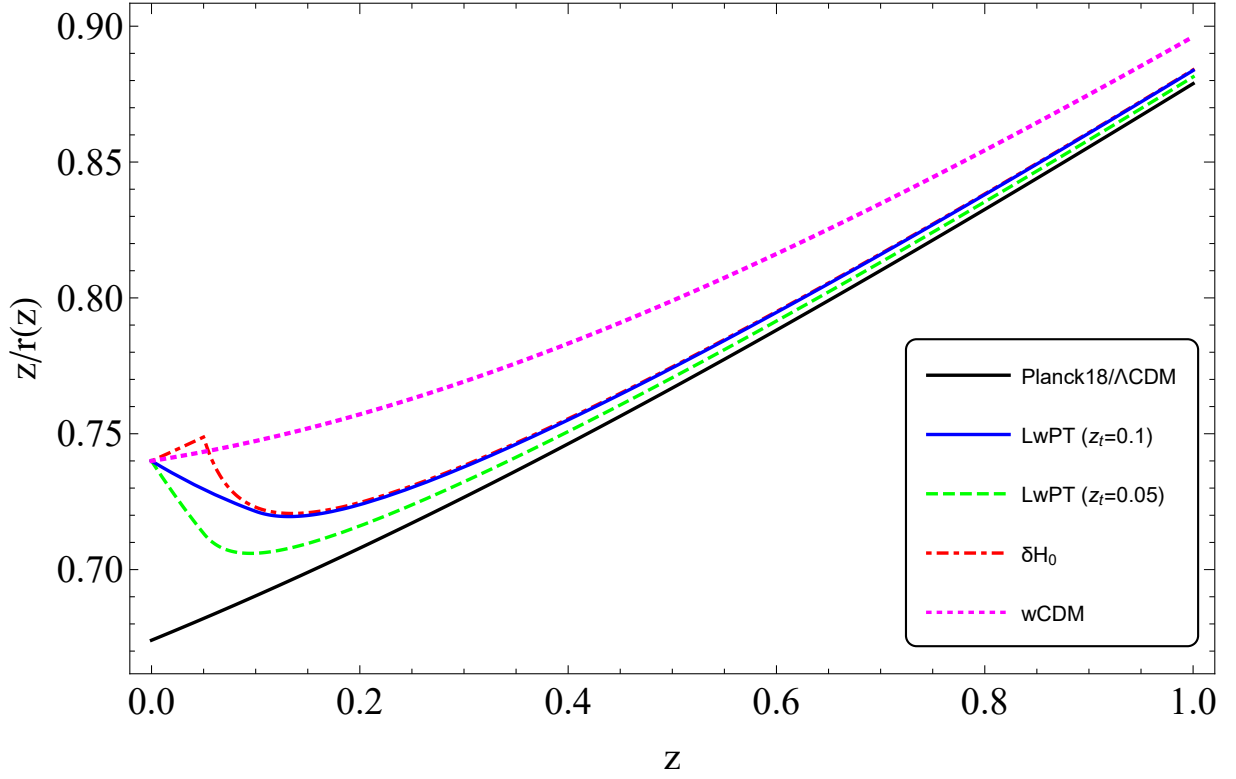


FIG. 2. The function $f(z) = z/r(z)$ where $r(z)$ is the comoving distance to redshift z for the cosmological models Planck18/ Λ CDM (black continuous line), w CDM with $w = -1.2$ (magenta dotted line), $H(z)$ transition (2.5) with $z_t = 0.05$ and $\delta = (h_{local} - h_{CMB})/h_{CMB}$ (red dot-dashed line), $LwPT$ with $z_t = 0.05$ and $w(z < z_t) = -1 - \Delta w = -2.78$ as indicated by eq. (2.4) (green dashed line) and $LwPT$ with $z_t = 0.1$ and $w(z < z_t) = -1 - \Delta w = -1.91$ as indicated by eq. (2.4) (blue continuous line). Notice that even though all three models approach $r_\Lambda(z)$ asymptotically, the two $LwPT$ models remain closest to the Planck18/ Λ CDM comoving distance $r_\Lambda(z)$ while at the same time they are consistent with the local measurement of the Hubble constant since $h_w(z=0) = 0.74$.

at $z = 0$ and decreases rapidly as z increases as demonstrated below.

The second condition imposes the constraint (2.2) on eq. (1.2) and leads to a relation between Δw and z_t of the form¹

$$\Delta w = \frac{\text{Log}(h^2 - \omega_m) - \text{Log}(h_{local}^2 - \omega_m)}{3\text{Log}(1 + z_t)} \quad (2.4)$$

where $h = h_{CMB} = 0.674$ and $\omega_m = \Omega_{0m}h^2 = 0.143$ as implied by the first condition and for consistency with the CMB anisotropy spectrum. In Fig. 1 we show a

plot of $\Delta w(z_t)$ demonstrating the strongly present day phantom behavior of dark energy implied by this class of models.

It is of interest to compare the form of the comoving distance $r(z)$ predicted in the context of the $LwPT$ model $r_w(z)$ with other proposed $H(z)$ deformations for the resolution of the Hubble tension. In Fig. 2 we show a plot of the function $f(z) \equiv z/r(z)$ (whose $z \rightarrow 0$ limit is the Hubble constant) for three proposed $H(z)$ deformation resolutions of the Hubble tension: the $LwPT$ model, the $H(z)$ transition model and the w CDM with fixed $w = -1.2$ model [42, 43, 45]. The $H(z)$ transition model is defined as

$$h_\delta(z)^2 \equiv (1 + \frac{\delta h}{h} \Theta(z_t - z))^2 [\omega_m(1+z)^3 + \omega_r(1+z)^4 + (h^2 - \omega_m - \omega_r)] \quad (2.5)$$

¹ Here we neglect ω_r as it has practically no effect on Δw .

where $\frac{\delta h}{h} = \frac{h_{local} - h_{CMB}}{h_{CMB}}$, $h = h_{CMB}$ and ω_m, ω_r are assumed fixed to their Planck18/ Λ CDM best fit values.

The fixed w ($wCDM$) smooth $H(z)$ deformation model is defined as

$$h_{wf}(z)^2 \equiv \omega_m(1+z)^3 + \omega_r(1+z)^4 + (h^2 - \omega_m - \omega_r)(1+z)^{3(1+w)} \quad (2.6)$$

where $w = -1.2$, $h = h_{local}$ and ω_m , ω_r are assumed fixed to their Planck18/ Λ CDM best fit values,

All three models that address the H_0 tension shown in Fig. 2 satisfy by construction two necessary conditions

$$h(z=0) = h_{local} \quad (2.7)$$

$$r(z) \rightarrow r_\Lambda(z) \text{ for } z \gtrsim O(1). \quad (2.8)$$

These conditions along with the fact that we fix the parameters ω_m and ω_r to their best fit Λ CDM values secure the fact that all three models produce the same CMB anisotropy spectrum as Planck18/ Λ CDM while at the same time they predict a Hubble parameter equal to its locally measured value $h(z=0) = h_{local}$. However, the three models do not approach the Planck18/ Λ CDM comoving distance $r_\Lambda(z)$ with the same efficiency as z increases. As is clearly seen in Fig. 2, the $LwPT$ model with both $z_t = 0.1$ and $z_t = 0.05$ approaches $r_\Lambda(z)$ faster than the other two models. Since Planck18/ Λ CDM provides an excellent fit to most geometric cosmological probes at $z > 0.1$ it is anticipated that $LwPT$ will produce a better fit to cosmological data than the smooth deformations of $H(z)$ like $wCDM$ or the discontinuous $H(z)$ transition model which produces an unnatural step in $r(z)$ and moves away from $r_\Lambda(z)$ for $z < z_t$ as z increases. This improved quality of fit is also demonstrated in the next section.

III. FITTING $LwPT$ TO COSMOLOGICAL DATA AND COMPARISON WITH $wCDM$

In this section we use a wide range of cosmological data to estimate the quality of fit and the best fit parameter values of three representative cosmological models:

- The $LwPT$ class of models defined by a Hubble expansion rate similar to that of eq. (1.2). Here we remove the constraint $w_{>} = -1$ for $z > z_t$ as well as the constraint $\omega_m = 0.143$. Thus the model is now allowed to have three free parameters for each fixed value of z_t : $w_{>}$, $w_{<} \equiv w_{>} + \Delta w$ and ω_m . However, as discussed below, the additional free parameters end up constrained by the data very close to the values considered fixed in the previous section. The constraint $h(z=0) = h_{local}$ is imposed as a prior in the analysis.
- The $wCDM$ model defined in (2.6) with two free parameters: w and ω_m . The constraint $h(z=0) = h_{local}$ is imposed as a prior in the analysis.

- The Λ CDM model defined by (2.6) with $w = -1$. No constraint for $h(z=0)$ is imposed on this model in order to maximize the quality of fit to the data and use the model as a benchmark for comparison with the other models that address the H_0 tension. Thus we use the term u Λ CDM (“u” for “unconstrained”) to denote it. It is considered as a baseline to compute residuals of χ^2 to compare the other two representative models. Its best fit parameter values in the context of the dataset we use are almost identical with Planck18/ Λ CDM ($\Omega_{0m} = 0.312 \pm 0.006$, $H_0 = 67.579 \pm 0.397$).

We use the following data to identify the quality of fit of these models

- The Pantheon SnIa dataset [54] consisting of 1048 distance modulus datapoints in the redshift range $z \in [0.01, 2.3]$.
- A compilation of 9 BAO datapoints in the redshift range $z \in [0.1, 2.34]$. The compilation is shown in the Appendix.
- The latest Planck18/ Λ CDM CMB distance prior data (shift parameter R [55] and the acoustic scale l_a [56]). These are highly constraining datapoints based on the observation of the sound horizon standard ruler at the last scattering surface $z \simeq 1100$. The covariance matrix of these datapoints and their values are shown in the Appendix.
- A compilation of 41 Cosmic Chronometer datapoints in the redshift range $z \in [0.1, 2.36]$. These datapoints are shown in the Appendix and have much less constraining power than the other data we use.

Using these data (total of 1100 datapoints) we used the maximum likelihood method [57] to minimize the total χ^2 defined as

$$\chi^2 = \chi_{CMB}^2 + \chi_{BAO}^2 + \chi_{CC}^2 + \chi_{Panth}^2 \quad (3.1)$$

and calculate the residual $\Delta\chi^2$ with respect to the u Λ CDM model for the $LwPT$ class (as a function of z_t) and for $wCDM$. Since the CMB data are the most constraining, we have found the anticipated best fits $\omega_m \simeq 0.143$ and $w = -1.22$ for $wCDM$ (see Ref. [42] for a detailed analysis of these results). In Fig. 3 we show the residuals $\Delta\chi^2$ for the best fit $LwPT$ models as a function of z_t (blue) and the corresponding residual $\Delta\chi^2$ for the best fit $wCDM$ model (horizontal black line). The

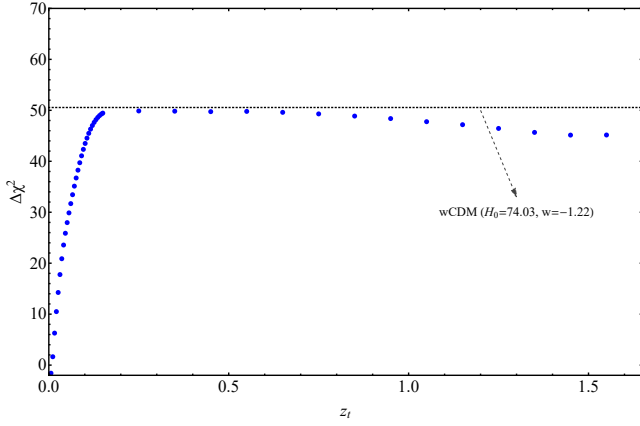


FIG. 3. The residuals $\Delta\chi^2$ plotted against the values of the transition redshift z_t for the $LwPT$ (blue dots) and $wCDM$ (black dotted line) with $w = -1.22$. The $LwPT$ model seems to achieve a significantly better fit for small z_t values.

rapid improvement of the fit compared to $wCDM$ for the $LwPT$ models as z_t decreases below $z_t \simeq 0.15$ is clear. The best fit parameter values for $w_<$ ($z < z_t$) and $w_>$ ($z > z_t$) are shown in Table I. In parenthesis next to each best fit we show the predicted value in the context of the analysis of the previous section (eq. (2.4)) which assumes $w_> = -1$.

TABLE I. The values of the $LwPT$ model best fit parameters Ω_{0m} , $w_<$ ($z < z_t$) and $w_>$ ($z > z_t$) corresponding to different indicative values of the transition redshift z_t , along with each case's $\Delta\chi^2$ with respect to ΛCDM . In parenthesis we show the analytically predicted values of $w_<$ which were obtained from eq. (2.4) (*i.e.* assuming $w_> = -1$ and imposing the constraint $h(z=0) = h_{local}$ on the $LwPT$ ansatz (1.2)). Notice that the best fit values of Ω_{0m} are consistent with the CMB spectrum requirement of $\omega_m = 0.143$ in view of the constraint $h(z=0) = h_{local}$ imposed in all cases.

z_t	$\Delta\chi^2$	Ω_{0m}	$w_< (z < z_t)$	$w_> (z > z_t)$
0.005	-1.9	0.2609	-18.44 (-18.4)	-1.005
0.01	0.8	0.2608	-9.93 (-9.7)	-1.001
0.02	9.7	0.2607	-5.28 (-5.3)	-1.011
0.04	23.1	0.2606	-2.93 (-3.2)	-1.037
0.05	27.6	0.2607	-2.48 (-2.8)	-1.049
0.06	31.3	0.2607	-2.19 (-2.5)	-1.059
0.08	37.9	0.2608	-1.81 (-2.1)	-1.085
0.1	43.3	0.2611	-1.58 (-1.9)	-1.115
0.2	50.1	0.2622	-1.22 (-1.4)	-1.23

The forms of the comoving Hubble parameter $H(z)/(1+z)$ for two $LwPT$ models with $z_t < 0.1$, the best fit $wCDM$ and ΛCDM are shown in Fig. 4. This figure demonstrates the efficiency of $LwPT$ in mimicking the best fit ΛCDM model (which is almost identical with Planck18/ ΛCDM) while at the same time addressing the Hubble tension by reaching $h(z=0) = h_{local}$ in a continuous manner. On the other hand the smoother approach of $wCDM$ is much less efficient in mimicking

Planck18/ ΛCDM and the price it pays for this inability is a much worse quality of fit compared to $LwPT$ as shown in Fig. 3.

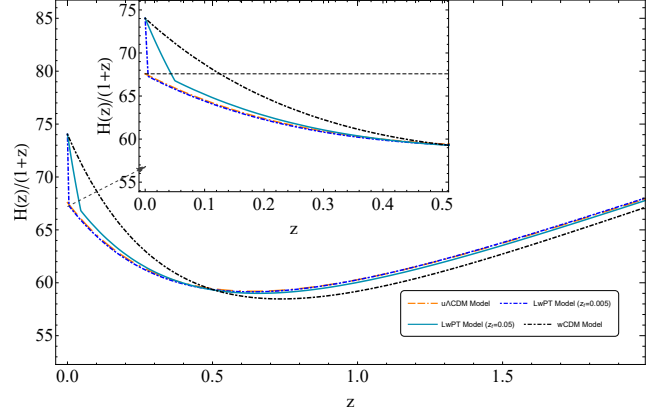


FIG. 4. The forms of the comoving Hubble parameter $H(z)/(1+z)$ for two $LwPT$ models with $z_t < 0.1$, the best fit $wCDM$ and ΛCDM .

The difficulty of the smooth $H(z)$ deformation models that address the Hubble tension in fitting the BAO and SnIa data is also demonstrated in Fig. 5 where we show the BAO and SnIa data (residuals from the best fit ΛCDM) along with the best fit residuals for the $wCDM$ and $LwPT$ models.

IV. CONCLUSION-DISCUSSION-OUTLOOK

We have demonstrated using both an analytical approach and a fit to cosmological data that a Late dark energy equation of state w Phantom Transition ($LwPT$) from $w_> = -1$ ($z > z_t$) to $w_< < -1$ ($z < z_t$) at transition redshift $z_t \in [0.01, 0.1]$ can lead to a resolution of the Hubble tension in a more efficient manner than smooth deformations of the Hubble tension and other types of late time transitions (the Hubble expansion rate transition). The required type of transition is a phantom transition with $w_<(z_t) \in [-2, -10]$ for $z < z_t$.

There is a wide range of physical models that can reproduce the $LwPT$. Such models include the following:

- The most natural model that can induce a $LwPT$ involves a phantom scalar field initially frozen at $\phi = \phi_0$ due to cosmic friction close to the zero point of its potential which could be assumed to be of the form $V(\phi) = s\phi^n$. Such a field would initially have a dark energy equation of state $w = -1$ mimicking a cosmological constant. Once Hubble friction becomes smaller than the field dynamical (mass) scale, the field becomes free to roll up its potential (phantom fields move up their potential in contrast to quintessence fields [58, 59]) and develops a rapidly changing equation of state parameter $w < -1$. Thus the universe enters a ghost instability phase which will end in a Big Rip singularity

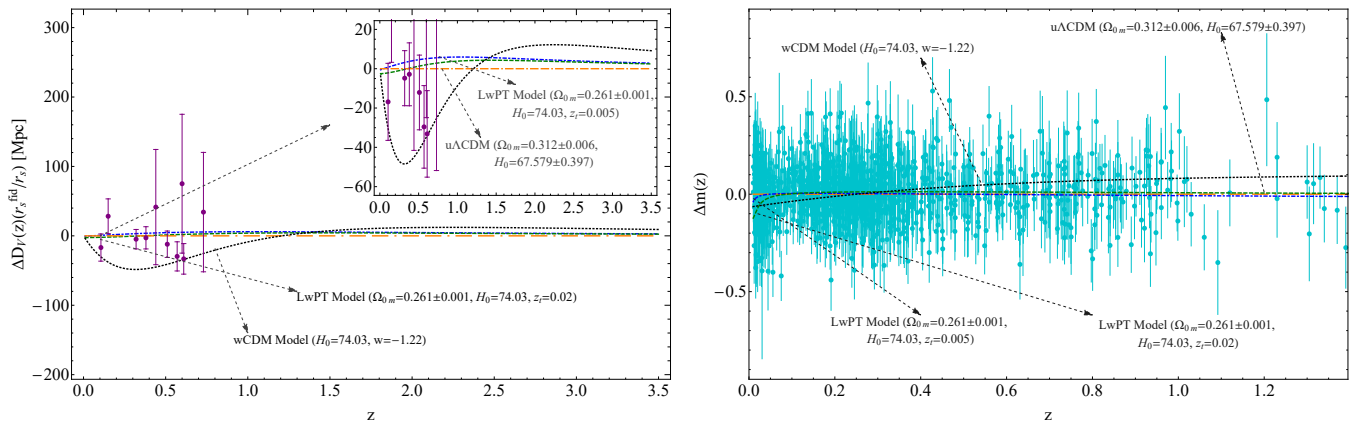


FIG. 5. *Left panel:* BAO data residuals $\Delta D_V \times \frac{r_s^{fid}}{r_s}$ from the best fit $u\Lambda$ CDM (orange dashed line) superimposed with the best fit residual curves corresponding to w CDM (dotted black line), $LwPT$ with $z_t = 0.005$ (blue dot dashed line) and $LwPT$ with $z_t = 0.02$ (green dashed line). Notice the difficulty of smooth $H(z)$ deformation of w CDM to fit the data due to the constraint imposed by the local measurements of Hubble constant. *Right panel:* The Pantheon SNIa distance modulus residuals Δm from the best fit $u\Lambda$ CDM. The predicted distance modulus residual curves for w CDM (black dashed line), the $LwPT$ ($z_t = 0.005$) (blue dot dashed line) and the $LwPT$ ($z_t = 0.02$) (green dashed line) are also shown.

in less than a Hubble time. Such a scenario for the simple (but also generic) case of linear potential ($n = 1$) has been investigated in Ref. [58]. For a general phantom potential we anticipate a redshift dependence of the equation of state $w_< = w_<(z)$ after the transition ($z < z_t$). In fact the phantom field potential could be reconstructed by demanding a form of $w_<(z)$ that further optimizes the quality of fit to the low z data or by simply demanding that $w_<$ is constant.

- A scalar-tensor modified gravity theory field initially frozen due to Hubble friction, mimicking general relativity and a cosmological constant. Once Hubble friction becomes smaller than the field mass scale, the field becomes free to roll down its potential inducing deviations from general relativity on cosmological scales and a phantom departure from the cosmological constant. Note that scalar tensor theories can induce phantom behavior without instabilities in contrast to a simple minimally coupled scalar field [60].
- A fluid with a nonstandard equation of state of the form $A\rho + Bp = (C\rho + Dp)^\alpha$ has been shown to exhibit a similar type of phantom transition from an initial state with $w = -1$ for $\alpha = 2$ [61].

The detailed investigation of the above described dynamical scalar field evolution that can reproduce the $LwPT$ is an interesting extension of the present analysis.

If the phantom $LwPT$ is realized in Nature it would imply the existence of a rapidly approaching Big Rip singularity [62, 63]. Given the value of $w_<$ which emerges at approximately the present time t_0 , it is straightforward to calculate the time t_* of the Big Rip singularity assuming that $w = w_< < -1$ at the present time t_0 . The result

is [63]

$$\frac{t_*}{t_0} = \frac{w_<}{1 + w_<} \quad (4.1)$$

For example for $z_t = 0.02$ we have $w_< \simeq -5$ which implies that the universe will end in a Big Rip singularity in less than 3.5 billion years (for $t_0 = 13.8 \times 10^9 \text{ yrs}$). This implies that there may be observational effects of such coming singularity on the largest bound systems like the Virgo cluster, the Coma Cluster or the Virgo supercluster. A detailed investigation of the observational effects on bound systems of the $LwPT$ is an interesting extension of the present analysis.

Another interesting extension of the present analysis is the detailed comparison of the quality of fit of the $LwPT$ models with a variety of other smooth $H(z)$ deformation models addressing the Hubble tension using also full CMB spectrum data.

Numerical Analysis Files: The numerical files for the reproduction of the figures can be found in [64].

ACKNOWLEDGEMENTS

We thank Savvas Nesseris for the useful discussions. LK's research is co-financed by Greece and the European Union (European Social Fund- ESF) through the Operational Programme "Human Resources Development, Education and Lifelong Learning" in the context of the project "Strengthening Human Resources Research Potential via Doctorate Research - 2nd Cycle" (MIS-5000432), implemented by the State Scholarships Foundation (IKY). LP's and GA's research is co-financed by Greece and the European Union (European Social Fund - ESF) through the Operational Programme "Human Resources Development, Education and Lifelong Learning

2014-2020” in the context of the project ”Scalar fields in Curved Spacetimes: Soliton Solutions, Observational Results and Gravitational Waves” (MIS 5047648).

eter R and the acoustic scale l_a), for a flat universe has the following form [56]

$$C_{ij} = 10^{-8} \times \begin{pmatrix} 1598.9554 & 17112.007 \\ 17112.007 & 811208.45 \end{pmatrix}$$

where the corresponding Planck18/ Λ CDM values for R and l_a are presented in Table II. Furthermore, we present the full dataset of the BAO and CC likelihoods used in the Mathematica analysis in Tables III and IV respectively.

Appendix A: Data Used in the Analysis

The covariance matrix which corresponds to the latest Planck18/ Λ CDM CMB distance prior data (shift param-

TABLE II: The CMB Distance Prior data for a flat Universe used in our analysis.

Index	CMB Observable	CMB Value	Reference
1	R	1.74963	[56]
2	l_a	301.80845	[56]

TABLE III: The BAO data that have been used in the analysis along with the corresponding references.

Index	z	D_A/r_s (Mpc)	D_H/r_s (km/sec Mpc)	D_V/r_s (Mpc)	Ref.
1	0.106	-	-	2.98 ± 0.13	[65]
2	0.44	-	-	13.69 ± 5.82	[66]
3	0.6	-	-	13.77 ± 3.11	[66]
4	0.73	-	-	16.89 ± 5.28	[66]
5	2.34	11.28 ± 0.65	-	-	[67]
6	2.34	-	9.18 ± 0.28	-	[67]
7	0.15	-	-	4.465 ± 0.168	[68]
8	0.32	-	-	8.62 ± 0.15	[69]
9	0.57	-	-	13.7 ± 0.12	[69]

TABLE IV: The Cosmic Chronometer data that have been used in the analysis.

Index	z	$H(z)$ (km/sec Mpc)	Ref.
1	0.09	69 ± 12	[70]
2	0.17	83 ± 8	[71]
3	0.179	75 ± 4	[72]
4	0.199	75 ± 5	[72]
5	0.27	77 ± 14	[71]
6	0.352	83 ± 14	[72]
7	0.3802	83 ± 13.5	[73]
8	0.4	95 ± 17	[71]
9	0.4004	77 ± 10.2	[73]
10	0.4247	87.1 ± 11.2	[73]
11	0.4497	92.8 ± 12.9	[73]
12	0.4783	80.9 ± 9	[73]
13	0.48	97 ± 62	[74]
14	0.593	104 ± 13	[72]
15	0.68	92 ± 8	[72]
16	0.781	105 ± 12	[72]
17	0.875	125 ± 17	[75]
18	0.88	90 ± 40	[74]
19	0.9	117 ± 23	[71]
20	1.037	154 ± 20	[72]
21	1.3	168 ± 17	[71]
22	1.363	160 ± 33.6	[76]
23	1.43	177 ± 18	[71]
24	1.53	140 ± 14	[71]

25	1.75	202 ± 40	[71]
26	1.965	186.5 ± 50.4	[76]
27	0.35	82.7 ± 8.4	[77]
28	0.44	82.6 ± 7.8	[78]
29	0.57	96.8 ± 3.4	[69]
30	0.6	87.9 ± 6.1	[78]
31	0.73	97.3 ± 7	[78]
32	2.34	222 ± 7	[79]
33	0.07	69 ± 19.6	[75]
34	0.12	68.6 ± 26.2	[75]
35	0.2	72.9 ± 29.6	[75]
36	0.24	79.69 ± 2.65	[80]
37	0.28	88.8 ± 36.6	[75]
38	0.43	86.45 ± 3.68	[80]
39	0.57	92.4 ± 4.5	[81]
40	2.3	224 ± 8	[82]
41	2.36	226 ± 8	[83]

-
- [1] Adam G. Riess, Stefano Casertano, Wenlong Yuan, Lucas M. Macri, and Dan Scolnic, “Large Magellanic Cloud Cepheid Standards Provide a 1% Foundation for the Determination of the Hubble Constant and Stronger Evidence for Physics beyond Λ CDM,” *Astrophys. J.* **876**, 85 (2019), [arXiv:1903.07603 \[astro-ph.CO\]](#).
- [2] Adam G. Riess *et al.*, “Milky Way Cepheid Standards for Measuring Cosmic Distances and Application to Gaia DR2: Implications for the Hubble Constant,” *Astrophys. J.* **861**, 126 (2018), [arXiv:1804.10655 \[astro-ph.CO\]](#).
- [3] Adam G. Riess *et al.*, “A 2.4% Determination of the Local Value of the Hubble Constant,” *Astrophys. J.* **826**, 56 (2016), [arXiv:1604.01424 \[astro-ph.CO\]](#).
- [4] Wendy L. Freedman, Barry F. Madore, Taylor Hoyt, In Sung Jang, Rachael Beaton, Myung Gyoon Lee, Andrew Monson, Jill Neeley, and Jeffrey Rich, “Calibration of the Tip of the Red Giant Branch (TRGB),” (2020), [10.3847/1538-4357/ab7339](#), [arXiv:2002.01550 \[astro-ph.GA\]](#).
- [5] Wendy L. Freedman *et al.*, “The Carnegie-Chicago Hubble Program. VIII. An Independent Determination of the Hubble Constant Based on the Tip of the Red Giant Branch,” (2019), [10.3847/1538-4357/ab2f73](#), [arXiv:1907.05922 \[astro-ph.CO\]](#).
- [6] D.W. Pesce *et al.*, “The Megamaser Cosmology Project. XIII. Combined Hubble constant constraints,” *Astrophys. J. Lett.* **891**, L1 (2020), [arXiv:2001.09213 \[astro-ph.CO\]](#).
- [7] N. Aghanim *et al.* (Planck), “Planck 2018 results. VI. Cosmological parameters,” *Astron. Astrophys.* **641**, A6 (2020), [arXiv:1807.06209 \[astro-ph.CO\]](#).
- [8] G.E. Addison, D.J. Watts, C.L. Bennett, M. Halpern, G. Hinshaw, and J.L. Weiland, “Elucidating Λ CDM: Impact of Baryon Acoustic Oscillation Measurements on the Hubble Constant Discrepancy,” *Astrophys. J.* **853**, 119 (2018), [arXiv:1707.06547 \[astro-ph.CO\]](#).
- [9] Nils Schöneberg, Julien Lesgourgues, and Deanna C. Hooper, “The BAO+BBN take on the Hubble tension,” *JCAP* **10**, 029 (2019), [arXiv:1907.11594 \[astro-ph.CO\]](#).
- [10] S. Birrer *et al.*, “H0LiCOW - IX. Cosmographic analysis of the doubly imaged quasar SDSS 1206+4332 and a new measurement of the Hubble constant,” *Mon. Not. Roy. Astron. Soc.* **484**, 4726 (2019), [arXiv:1809.01274 \[astro-ph.CO\]](#).
- [11] A.J. Shajib *et al.* (DES), “STRIDES: a 3.9 per cent measurement of the Hubble constant from the strong lens system DES J0408–5354,” *Mon. Not. Roy. Astron. Soc.* **494**, 6072–6102 (2020), [arXiv:1910.06306 \[astro-ph.CO\]](#).
- [12] B.P. Abbott *et al.* (LIGO Scientific, Virgo), “A gravitational-wave measurement of the Hubble constant following the second observing run of Advanced LIGO and Virgo,” (2019), [arXiv:1908.06060 \[astro-ph.CO\]](#).
- [13] M. Soares-Santos *et al.* (DES, LIGO Scientific, Virgo), “First Measurement of the Hubble Constant from a Dark Standard Siren using the Dark Energy Survey Galaxies and the LIGO/Virgo Binary–Black-hole Merger GW170814,” *Astrophys. J. Lett.* **876**, L7 (2019), [arXiv:1901.01540 \[astro-ph.CO\]](#).
- [14] Lloyd Knox and Marius Millea, “Hubble constant hunter’s guide,” *Phys. Rev. D* **101**, 043533 (2020), [arXiv:1908.03663 \[astro-ph.CO\]](#).
- [15] Edvard Mörtsell and Suhail Dhawan, “Does the Hubble constant tension call for new physics?” *JCAP* **09**, 025 (2018), [arXiv:1801.07260 \[astro-ph.CO\]](#).
- [16] G. Efstathiou, “A Lockdown Perspective on the Hubble Tension (with comments from the SH0ES team),” (2020), [arXiv:2007.10716 \[astro-ph.CO\]](#).
- [17] L. Kazantzidis and L. Perivolaropoulos, “Hints of a Local Matter Underdensity or Modified Gravity in the Low z Pantheon data,” *Phys. Rev. D* **102**, 023520 (2020), [arXiv:2004.02155 \[astro-ph.CO\]](#).
- [18] L. Kazantzidis, H. Koo, S. Nesseris, L. Perivolaropoulos, and A. Shafieloo, “Hints for possible low redshift oscillation around the best fit Λ CDM model in the expansion history of the universe,” (2020), [10.1093/mnras/staa3866](#), [arXiv:2010.03491 \[astro-ph.CO\]](#).
- [19] Domenico Sapone, Savvas Nesseris, and Carlos A.P. Bengaly, “Is there any measurable redshift dependence on the

- SN Ia absolute magnitude?” (2020), [arXiv:2006.05461 \[astro-ph.CO\]](#).
- [20] John Soltis, Stefano Casertano, and Adam G. Riess, “The Parallax of Omega Centauri Measured from Gaia EDR3 and a Direct, Geometric Calibration of the Tip of the Red Giant Branch and the Hubble Constant,” (2020), [arXiv:2012.09196 \[astro-ph.GA\]](#).
 - [21] Adam G. Riess, Stefano Casertano, Wenlong Yuan, J. Bradley Bowers, Lucas Macri, Joel C. Zinn, and Dan Scolnic, “Cosmic Distances Calibrated to 1% Precision with Gaia EDR3 Parallaxes and Hubble Space Telescope Photometry of 75 Milky Way Cepheids Confirm Tension with Λ CDM,” (2020), [arXiv:2012.08534 \[astro-ph.CO\]](#).
 - [22] Nikita Blinov, Kevin James Kelly, Gordan Z Krnjaic, and Samuel D McDermott, “Constraining the Self-Interacting Neutrino Interpretation of the Hubble Tension,” *Phys. Rev. Lett.* **123**, 191102 (2019), [arXiv:1905.02727 \[astro-ph.CO\]](#).
 - [23] Vivian Poulin, Tristan L. Smith, Tanvi Karwal, and Marc Kamionkowski, “Early Dark Energy Can Resolve The Hubble Tension,” *Phys. Rev. Lett.* **122**, 221301 (2019), [arXiv:1811.04083 \[astro-ph.CO\]](#).
 - [24] Jeremy Sakstein and Mark Trodden, “Early Dark Energy from Massive Neutrinos as a Natural Resolution of the Hubble Tension,” *Phys. Rev. Lett.* **124**, 161301 (2020), [arXiv:1911.11760 \[astro-ph.CO\]](#).
 - [25] Prateek Agrawal, Francis-Yan Cyr-Racine, David Pinner, and Lisa Randall, “Rock ‘n’ Roll Solutions to the Hubble Tension,” (2019), [arXiv:1904.01016 \[astro-ph.CO\]](#).
 - [26] Meng-Xiang Lin, Giampaolo Benevento, Wayne Hu, and Marco Raveri, “Acoustic Dark Energy: Potential Conversion of the Hubble Tension,” *Phys. Rev. D* **100**, 063542 (2019), [arXiv:1905.12618 \[astro-ph.CO\]](#).
 - [27] Matteo Braglia, William T. Emond, Fabio Finelli, A. Emir Gumrukcuoglu, and Kazuya Koyama, “Unified framework for Early Dark Energy from α -attractors,” (2020), [arXiv:2005.14053 \[astro-ph.CO\]](#).
 - [28] Florian Niedermann and Martin S. Sloth, “Resolving the Hubble Tension with New Early Dark Energy,” *Phys. Rev. D* **102**, 063527 (2020), [arXiv:2006.06686 \[astro-ph.CO\]](#).
 - [29] Tristan L. Smith, Vivian Poulin, José Luis Bernal, Kimberly K. Boddy, Marc Kamionkowski, and Riccardo Murgia, “Early dark energy is not excluded by current large-scale structure data,” (2020), [arXiv:2009.10740 \[astro-ph.CO\]](#).
 - [30] Balakrishna S. Haridasu, Matteo Viel, and Nicola Vittorio, “Sources of H_0 -tensions in dark energy scenarios,” (2020), [arXiv:2012.10324 \[astro-ph.CO\]](#).
 - [31] C. Krishnan, Eoin Ó. Colgáin, Ruchika, Anjan A. Sen, M.M. Sheikh-Jabbari, and Tao Yang, “Is there an early Universe solution to Hubble tension?” *Phys. Rev. D* **102**, 103525 (2020), [arXiv:2002.06044 \[astro-ph.CO\]](#).
 - [32] H. Hildebrandt *et al.*, “KiDS-450: Cosmological parameter constraints from tomographic weak gravitational lensing,” *Mon. Not. Roy. Astron. Soc.* **465**, 1454 (2017), [arXiv:1606.05338 \[astro-ph.CO\]](#).
 - [33] Shahab Joudaki *et al.*, “KiDS-450 + 2dFLenS: Cosmological parameter constraints from weak gravitational lensing tomography and overlapping redshift-space galaxy clustering,” *Mon. Not. Roy. Astron. Soc.* **474**, 4894–4924 (2018), [arXiv:1707.06627 \[astro-ph.CO\]](#).
 - [34] F. Köhlinger *et al.*, “KiDS-450: The tomographic weak lensing power spectrum and constraints on cosmological parameters,” *Mon. Not. Roy. Astron. Soc.* **471**, 4412–4435 (2017), [arXiv:1706.02892 \[astro-ph.CO\]](#).
 - [35] T.M.C. Abbott *et al.* (DES), “Dark Energy Survey year 1 results: Cosmological constraints from galaxy clustering and weak lensing,” *Phys. Rev. D* **98**, 043526 (2018), [arXiv:1708.01530 \[astro-ph.CO\]](#).
 - [36] Edward Macaulay, Ingunn Kathrine Wehus, and Hans Kristian Eriksen, “Lower Growth Rate from Recent Redshift Space Distortion Measurements than Expected from Planck,” *Phys. Rev. Lett.* **111**, 161301 (2013), [arXiv:1303.6583 \[astro-ph.CO\]](#).
 - [37] Lavrentios Kazantzidis and Leandros Perivolaropoulos, “Evolution of the $f\sigma_8$ tension with the Planck15/ Λ CDM determination and implications for modified gravity theories,” *Phys. Rev. D* **97**, 103503 (2018), [arXiv:1803.01337 \[astro-ph.CO\]](#).
 - [38] Savvas Nesseris, George Pantazis, and Leandros Perivolaropoulos, “Tension and constraints on modified gravity parametrizations of $G_{\text{eff}}(z)$ from growth rate and Planck data,” *Phys. Rev. D* **96**, 023542 (2017), [arXiv:1703.10538 \[astro-ph.CO\]](#).
 - [39] F. Skara and L. Perivolaropoulos, “Tension of the E_G statistic and redshift space distortion data with the Planck - Λ CDM model and implications for weakening gravity,” *Phys. Rev. D* **101**, 063521 (2020), [arXiv:1911.10609 \[astro-ph.CO\]](#).
 - [40] Lavrentios Kazantzidis and Leandros Perivolaropoulos, “Is gravity getting weaker at low z ? Observational evidence and theoretical implications,” (2019), [arXiv:1907.03176 \[astro-ph.CO\]](#).
 - [41] L. Kazantzidis, L. Perivolaropoulos, and F. Skara, “Constraining power of cosmological observables: blind redshift spots and optimal ranges,” *Phys. Rev. D* **99**, 063537 (2019), [arXiv:1812.05356 \[astro-ph.CO\]](#).
 - [42] G. Alestas, L. Kazantzidis, and L. Perivolaropoulos, “ H_0 tension, phantom dark energy, and cosmological parameter degeneracies,” *Phys. Rev. D* **101**, 123516 (2020), [arXiv:2004.08363 \[astro-ph.CO\]](#).
 - [43] Eleonora Di Valentino, Alessandro Melchiorri, and Joseph Silk, “Reconciling Planck with the local value of H_0 in extended parameter space,” *Phys. Lett. B* **761**, 242–246 (2016), [arXiv:1606.00634 \[astro-ph.CO\]](#).
 - [44] Tristan L. Smith, Vivian Poulin, and Mustafa A. Amin, “Oscillating scalar fields and the Hubble tension: a resolution with novel signatures,” *Phys. Rev. D* **101**, 063523 (2020), [arXiv:1908.06995 \[astro-ph.CO\]](#).
 - [45] Sunny Vagnozzi, “New physics in light of the H_0 tension: An alternative view,” *Phys. Rev. D* **102**, 023518 (2020), [arXiv:1907.07569 \[astro-ph.CO\]](#).
 - [46] Xiaolei Li and Arman Shafieloo, “A Simple Phenomenological Emergent Dark Energy Model can Resolve the Hubble Tension,” *Astrophys. J. Lett.* **883**, L3 (2019), [arXiv:1906.08275 \[astro-ph.CO\]](#).
 - [47] Eleonora Di Valentino, Ankan Mukherjee, and Anjan A. Sen, “Dark Energy with Phantom Crossing and the H_0 tension,” (2020), [arXiv:2005.12587 \[astro-ph.CO\]](#).
 - [48] Chethan Krishnan, Eoin O. Colgáin, M.M. Sheikh-Jabbari, and Tao Yang, “Running Hubble Tension and a H_0 Diagnostic,” (2020), [arXiv:2011.02858 \[astro-ph.CO\]](#).
 - [49] Michael J. Mortonson, Wayne Hu, and Dragan Huterer, “Hiding dark energy transitions at low redshift,” *Phys. Rev. D* **80**, 067301 (2009), [arXiv:0908.1408 \[astro-](#)

- ph.CO].
- [50] Giampaolo Benevento, Wayne Hu, and Marco Raveri, “Can Late Dark Energy Transitions Raise the Hubble constant?” *Phys. Rev. D* **101**, 103517 (2020), [arXiv:2002.11707 \[astro-ph.CO\]](#).
 - [51] S. Dhawan, D. Brout, D. Scolnic, A. Goobar, A.G. Riess, and V. Miranda, “Cosmological Model Insensitivity of Local H_0 from the Cepheid Distance Ladder,” *Astrophys. J.* **894**, 54 (2020), [arXiv:2001.09260 \[astro-ph.CO\]](#).
 - [52] Ryan E. Keeley, Shahab Joudaki, Manoj Kaplinghat, and David Kirkby, “Implications of a transition in the dark energy equation of state for the H_0 and σ_8 tensions,” *JCAP* **12**, 035 (2019), [arXiv:1905.10198 \[astro-ph.CO\]](#).
 - [53] Bruce A. Bassett, Martin Kunz, Joseph Silk, and Carlo Ungarelli, “A Late time transition in the cosmic dark energy?” *Mon. Not. Roy. Astron. Soc.* **336**, 1217–1222 (2002), [arXiv:astro-ph/0203383](#).
 - [54] D.M. Scolnic *et al.*, “The Complete Light-curve Sample of Spectroscopically Confirmed SNe Ia from Pan-STARRS1 and Cosmological Constraints from the Combined Pantheon Sample,” *Astrophys. J.* **859**, 101 (2018), [arXiv:1710.00845 \[astro-ph.CO\]](#).
 - [55] Oystein Elgaroy and Tuomas Multamäki, “On using the CMB shift parameter in tests of models of dark energy,” *Astron. Astrophys.* **471**, 65 (2007), [arXiv:astro-ph/0702343](#).
 - [56] Zhongxu Zhai and Yun Wang, “Robust and model-independent cosmological constraints from distance measurements,” *JCAP* **07**, 005 (2019), [arXiv:1811.07425 \[astro-ph.CO\]](#).
 - [57] Rubén Arjona, Wilmar Cardona, and Savvas Nesseris, “Unraveling the effective fluid approach for $f(R)$ models in the subhorizon approximation,” *Phys. Rev. D* **99**, 043516 (2019), [arXiv:1811.02469 \[astro-ph.CO\]](#).
 - [58] Leandros Perivolaropoulos, “Constraints on linear negative potentials in quintessence and phantom models from recent supernova data,” *Phys. Rev. D* **71**, 063503 (2005), [arXiv:astro-ph/0412308](#).
 - [59] S. Nesseris and Leandros Perivolaropoulos, “Crossing the Phantom Divide: Theoretical Implications and Observational Status,” *JCAP* **01**, 018 (2007), [arXiv:astro-ph/0610092](#).
 - [60] Leandros Perivolaropoulos, “Crossing the phantom divide barrier with scalar tensor theories,” *JCAP* **10**, 001 (2005), [arXiv:astro-ph/0504582](#).
 - [61] Hrvoje Stefancic, “Dark energy transition between quintessence and phantom regimes - An Equation of state analysis,” *Phys. Rev. D* **71**, 124036 (2005), [arXiv:astro-ph/0504518](#).
 - [62] Robert R. Caldwell, Marc Kamionkowski, and Nevin N. Weinberg, “Phantom energy and cosmic doomsday,” *Phys. Rev. Lett.* **91**, 071301 (2003), [arXiv:astro-ph/0302506](#).
 - [63] S. Nesseris and Leandros Perivolaropoulos, “The Fate of bound systems in phantom and quintessence cosmologies,” *Phys. Rev. D* **70**, 123529 (2004), [arXiv:astro-ph/0410309](#).
 - [64] <https://github.com/GeorgeAlestas/LwPT>.
 - [65] Florian Beutler, Chris Blake, Matthew Colless, D.Heath Jones, Lister Staveley-Smith, Lachlan Campbell, Quentin Parker, Will Saunders, and Fred Watson, “The 6dF Galaxy Survey: Baryon Acoustic Oscillations and the Local Hubble Constant,” *Mon. Not. Roy. Astron. Soc.* **416**, 3017–3032 (2011), [arXiv:1106.3366 \[astro-ph.CO\]](#).
 - [66] Chris Blake *et al.*, “The WiggleZ Dark Energy Survey: Joint measurements of the expansion and growth history at $z \leq 1$,” *Mon. Not. Roy. Astron. Soc.* **425**, 405–414 (2012), [arXiv:1204.3674 \[astro-ph.CO\]](#).
 - [67] Victoria de Sainte Agathe *et al.*, “Baryon acoustic oscillations at $z = 2.34$ from the correlations of Ly α absorption in eBOSS DR14,” *Astron. Astrophys.* **629**, A85 (2019), [arXiv:1904.03400 \[astro-ph.CO\]](#).
 - [68] Ashley J. Ross, Lado Samushia, Cullan Howlett, Will J. Percival, Angela Burden, and Marc Manera, “The clustering of the SDSS DR7 main Galaxy sample – I. A 4 per cent distance measure at $z = 0.15$,” *Mon. Not. Roy. Astron. Soc.* **449**, 835–847 (2015), [arXiv:1409.3242 \[astro-ph.CO\]](#).
 - [69] Lauren Anderson *et al.* (BOSS), “The clustering of galaxies in the SDSS-III Baryon Oscillation Spectroscopic Survey: baryon acoustic oscillations in the Data Releases 10 and 11 Galaxy samples,” *Mon. Not. Roy. Astron. Soc.* **441**, 24–62 (2014), [arXiv:1312.4877 \[astro-ph.CO\]](#).
 - [70] Raul Jimenez, Licia Verde, Tommaso Treu, and Daniel Stern, “Constraints on the equation of state of dark energy and the Hubble constant from stellar ages and the CMB,” *ArXiv e-prints* (2003), [10.1086/376595](#), [astro-ph/0302560](#).
 - [71] Joan Simon, Licia Verde, and Raul Jimenez, “Constraints on the redshift dependence of the dark energy potential,” *Phys. Rev. D* **71**, 123001 (2005).
 - [72] M Moresco, A Cimatti, R Jimenez, L Pozzetti, G Zamorani, M Bolzonella, J Dunlop, F Lamareille, M Mignoli, H Pearce, and et al., “Improved constraints on the expansion rate of the universe up to $z \sim 1.1$ from the spectroscopic evolution of cosmic chronometers,” *Journal of Cosmology and Astroparticle Physics* **2012**, 006–006 (2012).
 - [73] Michele Moresco, Lucia Pozzetti, Andrea Cimatti, Raul Jimenez, Claudia Maraston, Licia Verde, Daniel Thomas, Annalisa Citro, Rita Tojeiro, and David Wilkinson, “A 6% measurement of the Hubble parameter at $z \sim 0.45$: direct evidence of the epoch of cosmic re-acceleration,” *Journal of Cosmology and Astroparticle Physics* **2016**, 014 (2016).
 - [74] Daniel Stern, Raul Jimenez, Licia Verde, Marc Kamionkowski, and S. Adam Stanford, “Cosmic chronometers: constraining the equation of state of dark energy. I: $H(z)$ measurements,” *Journal of Cosmology and Astroparticle Physics* **2010**, 008 (2010).
 - [75] Cong Zhang, Han Zhang, Shuo Yuan, Siqi Liu, Tong-Jie Zhang, and Yan-Chun Sun, “Four New Observational $H(z)$ Data From Luminous Red Galaxies of Sloan Digital Sky Survey Data Release Seven,” *ArXiv e-prints* (2012), [10.1088/1674-4527/14/10/002](#), [1207.4541](#).
 - [76] Michele Moresco, “Raising the bar: new constraints on the Hubble parameter with cosmic chronometers at $z \sim 2$,” *Monthly Notices of the Royal Astronomical Society: Letters* **450**, L16–L20 (2015).
 - [77] Chia-Hsun Chuang and Yun Wang, “Modelling the anisotropic two-point galaxy correlation function on small scales and single-probe measurements of $H(z)$, $DA(z)$ and $f(z)\sigma_8(z)$ from the Sloan Digital Sky Survey DR7 luminous red galaxies,” *Monthly Notices of the Royal Astronomical Society* **435**, 255–262 (2013).
 - [78] Chris Blake *et al.*, “The WiggleZ Dark Energy Survey: joint measurements of the expansion and growth history

- at $z < 1$,” *Monthly Notices of the Royal Astronomical Society* **425**, 405–414 (2012).
- [79] Timothée Delubac et al., “Baryon acoustic oscillations in the Ly α forest of BOSS DR11 quasars,” *Astronomy & Astrophysics* **574**, A59 (2015).
 - [80] Enrique Gaztañaga, Anna Cabré, and Lam Hui, “Clustering of luminous red galaxies - iv. baryon acoustic peak in the line-of-sight direction and a direct measurement of $h(z)$,” *Monthly Notices of the Royal Astronomical Society* **399**, 1663–1680 (2009).
 - [81] Lado Samushia et al., “The clustering of galaxies in the SDSS-III DR9 Baryon Oscillation Spectroscopic Survey: testing deviations from Λ and general relativity using anisotropic clustering of galaxies,” *Monthly Notices of the Royal Astronomical Society* **429**, 1514–1528 (2013).
 - [82] N. G. Busca et al., “Baryon acoustic oscillations in the Ly α forest of BOSS quasars,” *Astronomy & Astrophysics* **552**, A96 (2013).
 - [83] Andreu Font-Ribera et al., “Quasar-lyman α forest cross-correlation from boss dr11: Baryon acoustic oscillations,” *Journal of Cosmology and Astroparticle Physics* **2014**, 027–027 (2014).